

## RECENT KEY CONTRIBUTIONS OF ICRF HEATING IN SUPPORT OF PLASMA SCENARIO DEVELOPMENT AND FAST ION STUDIES ON JET AND ASDEX UPGRADE

M.J. MANTSINEN  
Barcelona Supercomputing Center and ICREA  
Barcelona, Spain  
Email: [mervi.mantsinen@bsc.es](mailto:mervi.mantsinen@bsc.es)

D. GALLART, J. MANYER  
Barcelona Supercomputing Center  
Barcelona, Spain

C. CHALLIS, P. JACQUET, V. KIPTILY, M. SERTOLI, S. SHARAPOV, D. TAYLOR,  
CCFE, Culham Science Centre  
Abingdon, UK

R. BILATO, V. BOBKOV, A. KAPPATOU, R. OCHOUKOV, T. PÜTTERICH, P.A. SCHNEIDER,  
G. TARDINI, M. WEILAND  
Max-Planck-Institut für Plasmaphysik  
Garching, Germany

J. GALDON-QUIROGA, M. GARCIA-MUÑOZ, J. GONZALEZ-MARTIN  
Dept. of Atomic, Molecular and Nuclear Physics, Universidad de Sevilla  
Sevilla, Spain

YE.O. KAZAKOV, E. LERCHE, D. VAN EESTER  
Laboratory for Plasma Physics, LPP-ERM/KMS  
Brussels, Belgium

P. MANTICA, M. NOCENTE\*  
Institute for Plasma Science and Technology, National Research Council  
\*Also at: Dipartimento di Fisica "G. Occhialini", Università di Milano-Bicocca  
Milan, Italy

O. SAUTER  
Swiss Plasma Center, EPFL-SPC  
Lausanne, Switzerland

### JET CONTRIBUTORS

See the author list of 'Overview of JET results for optimising ITER operation' by J. Mailloux *et al.* to be published in Nuclear Fusion Special issue: Overview and Summary Papers from the 28<sup>th</sup> Fusion Energy Conference (Nice, France, 10-15 May 2021)

### EUROFUSION MST1 TEAM

See the author list of B. Labit et al., 2019 Nucl. Fusion 59 086020.

### ASDEX UPGRADE TEAM

See the author list of H. Meyer et al., 2019 Nucl. Fusion 59 112014.

### Abstract

Ion Cyclotron Resonance Frequency (ICRF) heating plays an important role in many present day experiments and it is one of the auxiliary heating methods that will be used in ITER. This paper reports on recent ICRF experiments carried out in H-mode and improved confinement regimes on the JET and ASDEX Upgrade (AUG) tokamaks to further consolidate the ICRF physics basis for ITER. The design of all the experiments has been guided by ICRF modelling, which has allowed the identification of the most suitable experimental configuration to obtain and/or observe the desired effects. First, <sup>3</sup>He minority heating, which is one of the main ICRF scenarios at the full magnetic field of 5.3 T in ITER deuterium-tritium plasmas, has been investigated in JET high-performance hybrid target plasmas as well as AUG H-mode plasmas. The experiments were carried out in deuterium and will be expanded to deuterium-tritium and pure tritium isotope mixtures in the forthcoming JET

campaigns. Second, new ICRF scenarios have been developed and tested on AUG to expand the parameter space for ITER relevant studies on AUG. This work has included second harmonic heating of hydrogen to provide central ICRF power deposition in ITER-like baseline like plasma scenario on AUG. The scheme has been compared and used in conjunction with the standard hydrogen minority heating. One of the advantages of using second harmonic heating of hydrogen is that it allows the use of ICRF heating in ITER relevant plasma scenario studies on AUG at lower magnetic fields than would be otherwise possible. Finally, third harmonic ICRF heating of D beam ions has been developed on AUG to provide a new tool to create very energetic ICRF-accelerated fast deuteron populations for fast ion studies as well as for testing fast ion and fusion product related diagnostics. Selected discharges have been modelled with ICRF modelling tools which has provided invaluable test cases for their experimental validation as well as supported the analysis of the experimental results.

## 1. INTRODUCTION

Heating with waves in the ion cyclotron range of frequencies (ICRF) is a well-established method and it plays a key role in the operation and plasma performance optimization in many present-day fusion devices. One of the main aims of the current fusion research is to understand plasma behaviour in devices with metallic high-Z plasma facing components similar to those in ITER. It has turned out that ICRF heating can have beneficial effects in such devices by altering plasma impurity behaviour as well as plasma transport properties in a number of ways [1]. This has opened the door for some degree of ICRF optimization depending on the plasma characteristics and the ICRF system capabilities. The present paper reports on recent experiments carried out on the JET and ASDEX Upgrade (AUG) tokamaks with high-Z plasma facing components to develop and investigate ICRF schemes and plasma scenarios with relevance to ITER. The design of these experiments has been guided by extensive ICRF modelling, which has allowed the identification of the most suitable experimental configuration to obtain and/or observe the desired effects. Table 1 summarizes the ICRF schemes and plasma scenarios considered.

In JET experiments, the focus has been in the preparation of integrated scenarios for high fusion performance with long duration ( $P_{\text{fus}}=15\text{MW}$  for 5s) [2] and alpha physics [3] in the forthcoming campaign with deuterium-tritium (D-T) fuel mixture. Following the successful earlier characterization and optimization of hydrogen minority heating for the use in JET scenario plasmas [4], the new JET developments reported here have aimed for the integration of  $^3\text{He}$  minority heating in high-performance D plasmas for improved bulk ion heating compatible with the control of central high-Z impurity accumulation in the presence of the ITER-like metallic wall. As part of these studies, we have tested dual frequency ICRF heating consisting of combined H and  $^3\text{He}$  minority heating. This combination has maximized the available ICRF power from the presently available JET ICRF system at high magnetic fields of 3.4 T and above, which is particularly relevant for high-performance plasma scenario development.

$^3\text{He}$  minority heating is of interest for ITER because it coincides, for a given magnetic field and ICRF frequency, with second harmonic heating of tritium which is the standard ICRF heating scenario in ITER deuterium-tritium plasmas at the full magnetic field of 5.3T. Using small amounts of  $^3\text{He}$  minority ions in the ITER plasma can provide an additional means to optimize the performance characteristics of this ICRF scenario. This may become relevant e.g. in the plasma ramp up phase when the fast tritium tail ions may become too energetic for efficient bulk ion heating. Bulk ion heating is one of the unique properties of ICRF heating in ITER. In fact, it is foreseen that ICRF heating will be the only scheme among the auxiliary heating schemes envisaged in ITER that can provide dominant bulk ion heating. The other heating methods in ITER, i.e. heating with electron cyclotron waves and neutral beam injection of MeV-energy-range ions, will provide mainly electron heating. In the recent JET experiments, the main aim was to integrate and characterize  $^3\text{He}$  minority heating in the high-performance discharges in preparation of its use in ITER while the experiments with  $^3\text{He}$  minority heating on AUG focused on the plasma transport studies in the presence of bulk ion heating provided by this ICRF scheme. The experiments demonstrated that dominant bulk ion heating by ICRF waves is compatible with high-Z impurity control in the device with metallic high-Z plasma facing components.

TABLE 1. SUMMARY OF ICRF SCHEMES AND PLASMA SCENARIOS IN JET AND AUG INCLUDED IN THE PRESENT PAPER.

Device	ICRF scheme	Plasma scenario
JET	$^3\text{He}$ minority heating	High-performance hybrid
JET	Dual frequency $^3\text{He}$ minority +H minority heating	High-performance hybrid
AUG	$^3\text{He}$ minority heating	H mode
AUG	2nd harmonic H+H minority heating	ITER baseline like
AUG	Third harmonic heating of D	H mode

As shown in Table 1, the paper will also report on experiments carried out on AUG with fundamental and second harmonic heating of hydrogen in ITER baseline relevant plasmas as well as third harmonic heating of deuterium in H mode plasmas. Such novel applications of ICRF waves for plasma heating have recently become possible thanks to the improved operating space of ICRF system and, in particular, its extended frequency range [5]. The application of second harmonic heating of hydrogen on AUG allows for improved core electron heating in the ITER-baseline-like plasmas with pure wave heating (i.e. without NBI-induced torque to simulate ITER burning plasma conditions) [6]. The extended frequency range has also been instrumental for the experiments using third harmonic ICRF heating of NBI-injected deuterons for fast ion studies and for further development of fast ion and neutron diagnostics.

The variety of new ICRF scenarios in the two devices of different sizes considered here has provided a test bed for the validation of numerous modelling tools. In this paper we will use ICRF modelling code PION [7] to analyse the experimental results. PION computes the ICRF power absorption and the distribution functions of the resonant ions in a self-consistent way. Thanks to its speed, it forms a part of the automated data processing chain at JET, and has recently been installed in the ITER Integrated Modelling and Analysis Suite (IMAS) for integrated predictive modelling of ITER. Despite its relatively simple physics model, we find that PION is broadly consistent with many features observed in the experiments such as power partitioning between bulk ions and electrons and neutron production due to ICRF-accelerated deuterons.

The rest of this paper is organized as follows: In Section 2 the JET experiments with  $^3\text{He}$  minority heating and combined  $^3\text{He}$  and hydrogen minority heating are presented. In Section 3 the AUG experiments are presented including some recent key results with  $^3\text{He}$  minority heating, 2nd harmonic heating of H with and without H minority heating and third harmonic heating of D beam ions. Finally, Section 4 provides the conclusions.

## 2. $^3\text{He}$ MINORITY HEATING ON THE JET TOKAMAK

The experiments with  $^3\text{He}$  minority heating in JET high-performance hybrid discharges were carried out with deuterium as the main ion species at a magnetic field of 3.4 T and a plasma current of 2.2 MA. Up to 5 MW of ICRF power with an ICRF frequency of 33 MHz was applied. NBI power was in the range of 22 MW. The  $^3\text{He}$  concentration was increased gradually from 0% up to 8% of the electron density from discharge to discharge. Figure 1 shows the time evolution of discharges 94671 and 94674 with  $^3\text{He}$  minority heating together with those in 3.3 T/ 2.2 MA reference discharge 94667 with more standard H minority heating using an ICRF frequency of 42 MHz. As we can see, the discharges with  $^3\text{He}$  minority heating reach a higher plasma temperature and neutron rate while maintaining a lower plasma density. This is due to a lower core tungsten density in discharges with  $^3\text{He}$  minority heating observed throughout the  $^3\text{He}$  scan. Figure 2 shows a comparison of two discharges to illustrate the differences in the tungsten concentration at different flux surfaces in discharge 94669 with H minority and discharge 94672 with  $^3\text{He}$  minority. As we can see from Fig. 2, the central tungsten concentration is reduced by factor of 2-3 with  $^3\text{He}$  minority heating as compared to H minority heating.

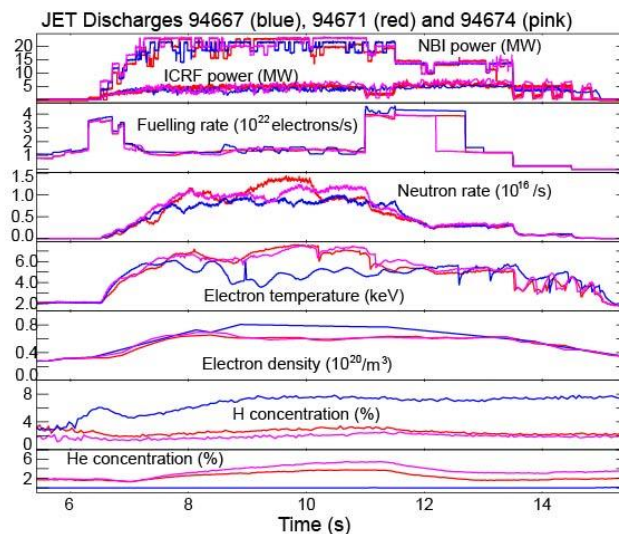


Fig. 1 Time evolution of main plasma parameters in 3.3 T/ 2.2 MA discharges 94671 (red) and 94674 (pink) with  $^3\text{He}$  minority heating together with those in 3.3 T/ 2.2 MA discharge 94667 (blue) with H minority heating.

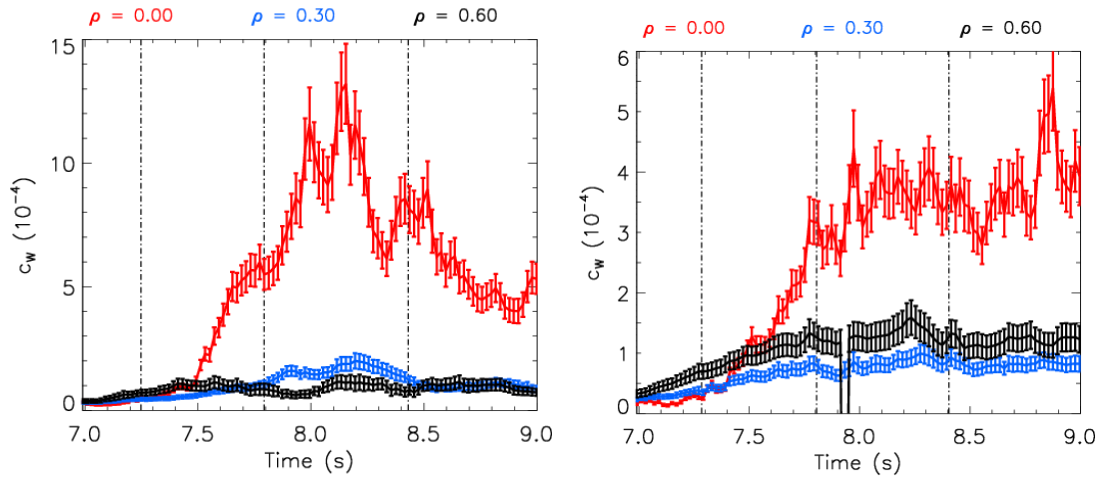


Fig. 2. Time evolution of the tungsten concentration for flux surfaces  $\rho = 0, 0.3$  and  $0.6$  in discharge 94669 with H minority heating (left) and discharge 94672 with  $^3\text{He}$  minority heating (right). Note the difference in the scale of the vertical axes.

Figure 3 shows the variation of the neutron rate as a function of  $^3\text{He}$  minority concentration for the discharges in the scan. Also, the neutron rates obtained with standard H minority heating in similar discharges are shown. The highest neutron rates with  $^3\text{He}$  minority heating and H minority heating are similar while there is a difference in the thermal and non-thermal neutron rates given the fact that the neutron rate with H minority heating is enhanced typically by 10-20% by ICRF-acceleration of NBI-injected deuterons which does not take place with  $^3\text{He}$  minority heating. As we can see from Fig. 3, the best plasma performance in terms of the neutron rate is obtained at a low  $^3\text{He}$  concentration of  $\sim 2\%$ , which also coincides with the best plasma temperature and plasma energy content. This result is encouraging for ITER as a low  $^3\text{He}$  concentration is advantageous in light of a modest  $^3\text{He}$  consumption and thereby a lower operational cost when using  $^3\text{He}$  minority heating in ITER. The result is also well in line with earlier computational multi-code work [8] for ITER where good absorption performance with a  $^3\text{He}$  concentration of  $\sim 3\%$  was found.

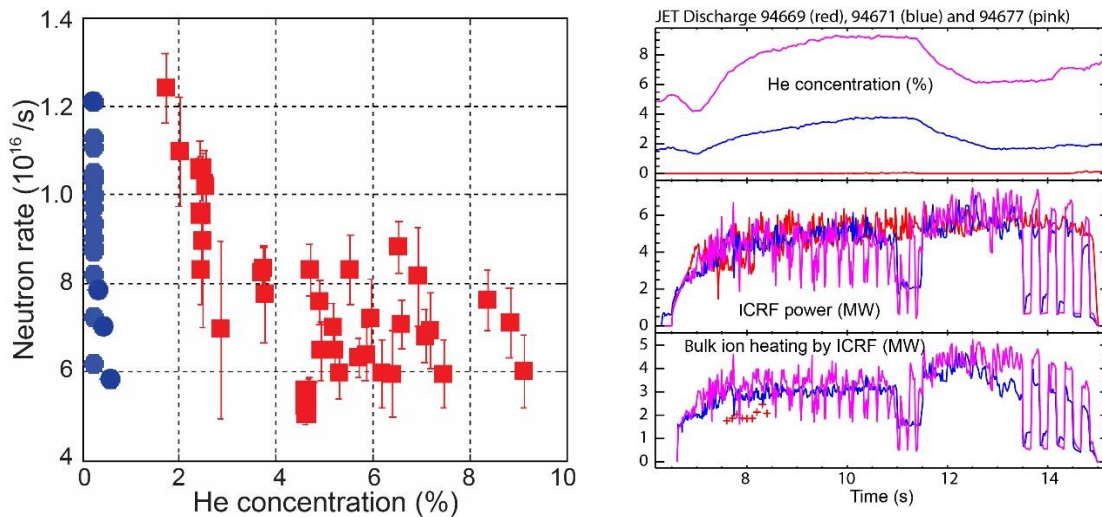


Fig. 3. Neutron rate as a function of  $^3\text{He}$  minority concentration in discharges with  $^3\text{He}$  minority heating (red) and in discharges with H minority heating (blue).

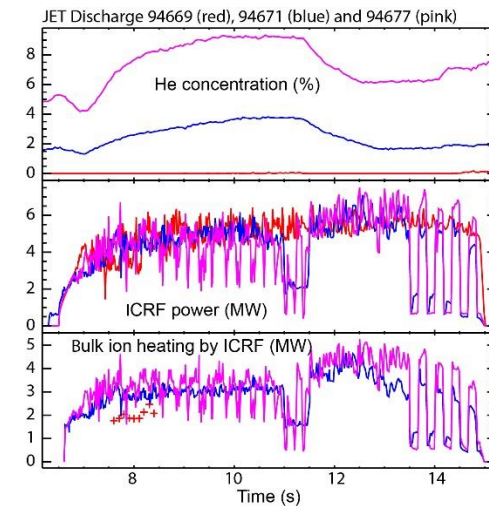


Fig. 4 He concentration, ICRF power and bulk ion heating power due to ICRF in JET discharge 94669 with H minority heating and in JET discharges 94671 and 94677 with  $^3\text{He}$  minority heating.

In the JET experiments we also confirmed experimentally that adding  $\sim 2\%$  of  $^3\text{He}$  in a hybrid plasma heated by a combination of deuterium NBI and H minority ICRF heating has a minimal effect on the performance, impurity behavior, pedestal and ELMs. Thus, the experimental differences between H minority heating and  $^3\text{He}$  minority heating with a low  $^3\text{He}$  concentration of a few % are due to changes in the ICRF heating characteristics rather than changes in the plasma composition or changes in wall sputtering or recycling due to added  $^3\text{He}$ . Furthermore,

ICRF modelling with PION confirms that in these plasma conditions,  $^3\text{He}$  minority heating produces stronger bulk ion heating and weaker fast ion population than H minority heating as shown in Fig 4. These differences can alter plasma transport properties in various ways (via changes in plasma profiles, collisionality, impurity screening, etc), leading to the differences observed in the overall plasma behaviour.

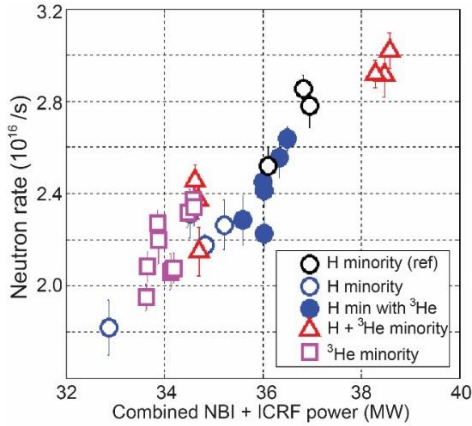


Fig. 5 Neutron rate as a function combined ICRF and NBI power in discharges with different ICRF schemes: H minority heating (circles),  $^3\text{He}$  minority heating (squares) and combined H and  $^3\text{He}$  minority heating (triangles).

Finally, we have tested dual frequency ICRF operation with combined H and  $^3\text{He}$  heating in JET hybrid plasmas. Dual frequency operation has the advantage of maximizing the coupled ICRF power from the JET ICRF antennas for magnetic fields above 3.4 T. With dual frequency operation at 3.4 T an ICRF power of  $\sim 8$  MW was demonstrated, which yielded an enhanced combined NBI and ICRF power and thereby, as shown in Figure 5, significantly improved plasma performance with respect to the other schemes with less coupled ICRF power. We can also see in Fig 5 that the neutron rate in the JET hybrid plasmas scales roughly linearly with combined NBI and ICRF power, which makes the total input power a key ingredient for maximizing the plasma fusion performance. In the coming JET campaigns, which will include a campaign with tritium and D-T plasmas, these experiments will be extended to the studies of  $^3\text{He}$  minority heating and second harmonic heating of tritium, which are the two main ICRF heating schemes planned for ITER full-field operation in 50%-50% D-T plasmas.

### 3. EXPERIMENTS ON THE ASDEX UPGRADE TOKAMAK

In this Section we discuss experiments carried out on AUG with  $^3\text{He}$  minority heating, 2nd harmonic heating of H with and without H minority heating and third harmonic heating of D beam ions. These experiments continue our earlier studies [6, 9, 12] and have been one of the drivers to the recent enhancements in the operational space of ICRF system and, in particular, in its frequency range on AUG [5].

#### 3.1 $^3\text{He}$ minority heating on AUG

The recent experiments with  $^3\text{He}$  minority heating on AUG have continued earlier experiments with this ICRF heating scheme which resulted in strongly peaked ion temperature profiles together with peaked x-ray emission profiles indicating tungsten density peaking in the plasma core [9]. The experiments were carried out at a magnetic field of 2.75-3T, a plasma current of 0.6 MA, electron density of about  $6 \times 10^{19} \text{m}^{-3}$  with NBI power of about 5 MW and ICRF power of about 4 MW. The new experiments were carried out with the aim to clarify the role of impurity peaking in the ion temperature peaking. The new discharges were prepared in the same way as the earlier discharges except for the application of prior wall conditioning with boronization in order to reduce impurity sources. In the new discharges similar peaked  $T_i$  profiles were obtained as in the earlier discharges while there was no soft x-ray radiation peaking. This is illustrated by Figures 6 and 7 which show the radial ion temperature profiles and soft x-ray (SXR) radiation peaking factor for discharge 37886 and reference discharge 31563 with and without prior wall conditioning, respectively. Here, the SXR peaking factor has been calculated as the ratio of the SXR radiation in the central channel to that of a channel viewing the plasma at mid-radius. These experiments thus demonstrate that radiation and impurity peaking do not play a major role in the ion temperature peaking in the present experimental conditions on AUG. ICRF modelling with PION confirms dominant bulk ion heating which central power deposition, which is consistent with the high ion temperatures reached in these discharges. Moreover, nonlinear electromagnetic stabilization of ion-temperature gradient microturbulence by fast  $^3\text{He}$  ions could also have played a role [10, 11].

#### 3.1 Second harmonic heating of hydrogen on AUG

In our earlier works [6, 12], we explored, both experimentally and with modelling, the viability of pure wave heating to simulate heating by fusion-born alpha particles without NBI-induced torque in ITER baseline relevant plasmas on AUG. We concluded that, instead of standard H minority ICRF heating, central second harmonic ICRF heating of H minority in combination of ECRF heating could lead to improved core electron heating [6]. As next step, we have carried out discharges where central second harmonic H minority heating was applied alone

and in combination of off-axis H minority heating and compared with pure off-axis H minority heating. Figure 8 shows the time-evolution of the main plasma parameters in discharge 36144 carried out at a magnetic field of 1.8 T, a plasma current of 1.1 MA and an electron density of  $\approx 6.35 \times 10^{19} \text{ m}^{-3}$ . While NBI power was kept constant at 4 MW and no ECRF was applied, a sequence of three phases with different ICRH schemes were programmed with the same ICRF power of 1.5 MW, i.e. one phase with H minority heating with an ICRF frequency of 30 MHz, one phase with second harmonic heating of H with an ICRF frequency of 55.1 MHz, and one phase with dual ICRF frequencies of 30 and 55.1 MHz for combined H minority heating and second harmonic heating of H. As we can see, second harmonic heating of hydrogen results in a slightly higher electron temperature, normalized plasma beta and fusion yield as compared to H minority heating or dual ICRF frequency operation, which is consistent with the theoretical expectations based on ICRF modelling carried out with PION.

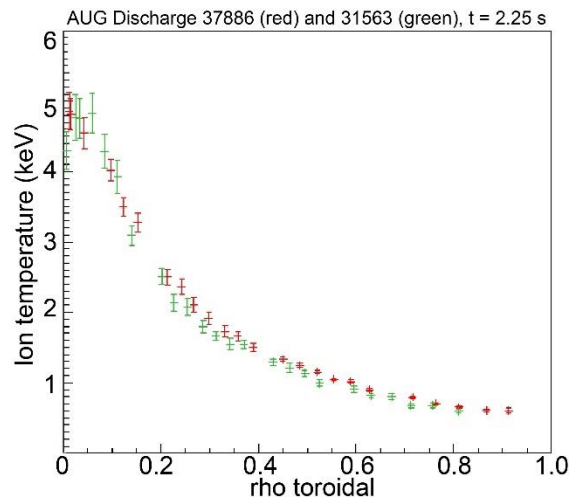


Fig. 6. Radial ion temperature profile for discharges 37886 and 31563 with  $^3\text{He}$  minority heating with and without prior wall conditioning with boronization, respectively.

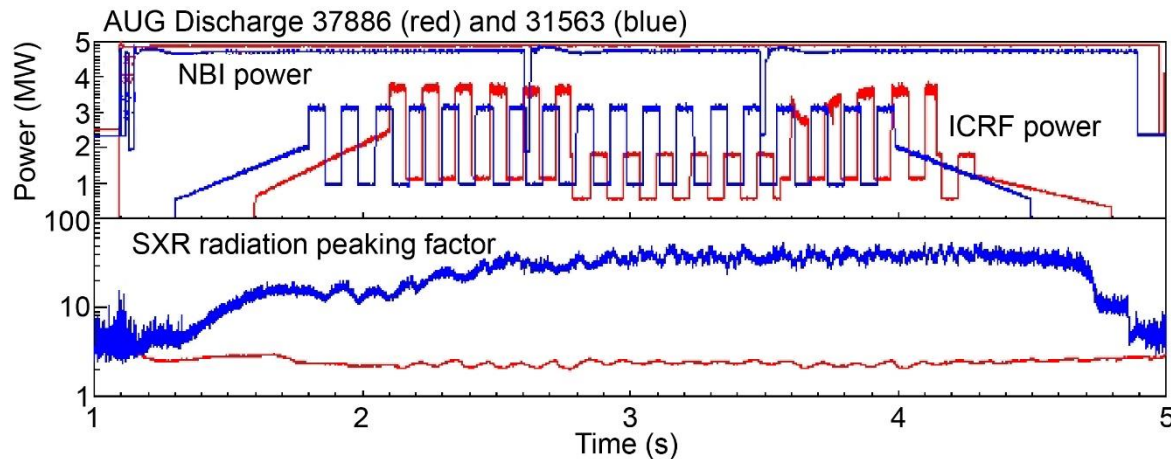


Fig. 7. Time evolution of NBI and ICRF power and the radiation peaking factor deduced from soft X-ray (SXR) measurements for discharges 37886 and 31563 with  $^3\text{He}$  minority heating and with and without prior wall conditioning with boronization, respectively.

### 3.3 Third harmonic heating of deuterium in synergy with deuterium beam injection on AUG

The extended frequency range on AUG has also been instrumental for the experiments using third harmonic ICRF heating of NBI-injected deuterons for fast ion studies and for further development of fast ion and neutron diagnostics. The recent experiments successfully extended our earlier work with this ICRF scheme on AUG at a magnetic field of about 1.8 T [13] to more robust plasmas with central ECRF heating at a magnetic field in the range of about 2.5 T. Figure 9 shows the time evolution of the main plasma parameters for discharge 35489 with third harmonic ICRF heating of deuterium with synergy with D NBI, displaying a more than two-fold increase of the D-D fusion rate as well as lengthening of the sawtooth period due to ICRF-accelerated deuterons. Controlled

variations of the fast D distribution were demonstrated in these experiments in response to variations in several physical parameters such as NBI, ICRF power, the background electron temperature, and ICRF resonance location, in line with theoretical predictions. Information on fast deuteron populations was obtained with an array of diagnostics including neutral particle analysers, fast ion loss detectors, neutron diagnostics and ion cyclotron emission (ICE) probe in the energy range of several tens of keVs to MeVs relevant for fusion-born alpha particles.

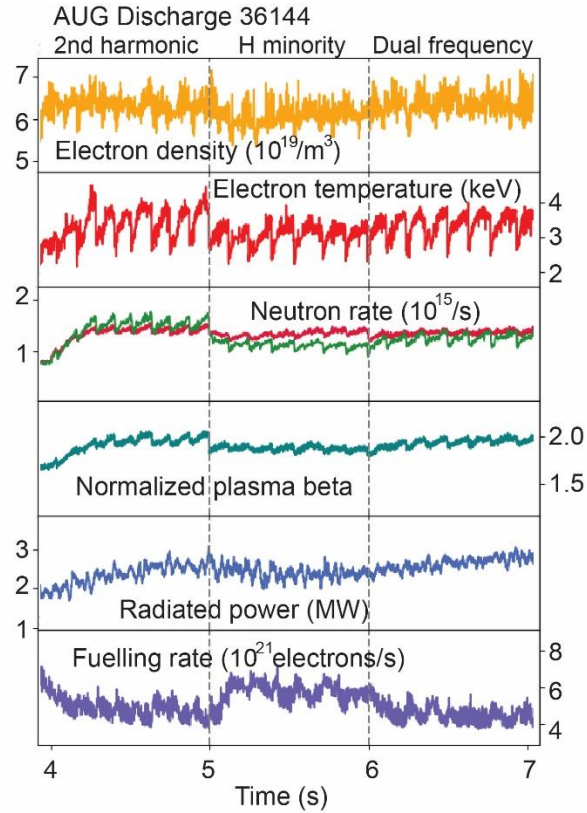


Fig. 8. Time evolution of electron density, electron temperature, neutron rate measured with two different diagnostics, plasma normalized beta, radiated power and fuelling rate for AUG discharge 36144 during three different phases of ICRF heating, i.e. first phase with second harmonic heating of H with an ICRF frequency of 55.1 MHz, second phase with H minority heating with an ICRF frequency of 30.0 MHz, and third phase with dual ICRF frequencies of 30 and 55.1 MHz for combined H minority heating and second harmonic heating of H.

#### 4. CONCLUSIONS

Heating with ICRF waves is a well-established method on present-day tokamaks and one of the heating systems foreseen for ITER. Moreover, it is the only scheme that can predominantly heat bulk ions in ITER. This paper reported on recent ICRF experiments carried out in H-mode and improved confinement regimes on the JET and ASDEX Upgrade (AUG) tokamaks to further consolidate the ICRF physics basis for ITER. The design of all the experiments has been guided by ICRF modelling, which has allowed the identification of the most suitable experimental configuration to obtain and/or observe the desired effects. First, experiments were carried out on JET high-performance hybrid scenario plasmas to evaluate the respective merits of H,  $^3\text{He}$  and mixed ICRH schemes for scenario usage. The experiments were carried out in deuterium and will be expanded to deuterium-tritium and pure tritium isotope mixtures in the forthcoming JET campaigns. Second, new ICRF scenarios have been developed and tested on AUG to expand the parameter space for ITER relevant studies on AUG. This work has included a study of the role of impurity density peaking on the ion temperature peaking with  $^3\text{He}$  minority heating as well as the development of second harmonic heating of hydrogen to provide central ICRF power deposition in ITER-like baseline like plasma scenario on AUG. The latter scheme was compared and used in conjunction with the standard hydrogen minority heating. The advantage of using second harmonic heating of hydrogen is that it allows ICRF heating in ITER relevant plasma scenario studies on AUG at lower magnetic fields than would be otherwise possible. Finally, third harmonic ICRF heating of D beam ions has been developed on AUG to provide a new tool to create very energetic ICRF-accelerated fast deuteron populations for fast ion studies as well as for testing fast ion and fusion product related diagnostics. Selected discharges were modelled with ICRF modelling tools which has provided test cases for their experimental validation as well as supported

the analysis of the experimental results. The results obtained increase our confidence in the applications of PION [7] for predictive simulations of future experiments planned in the JET D-T campaign and ITER.

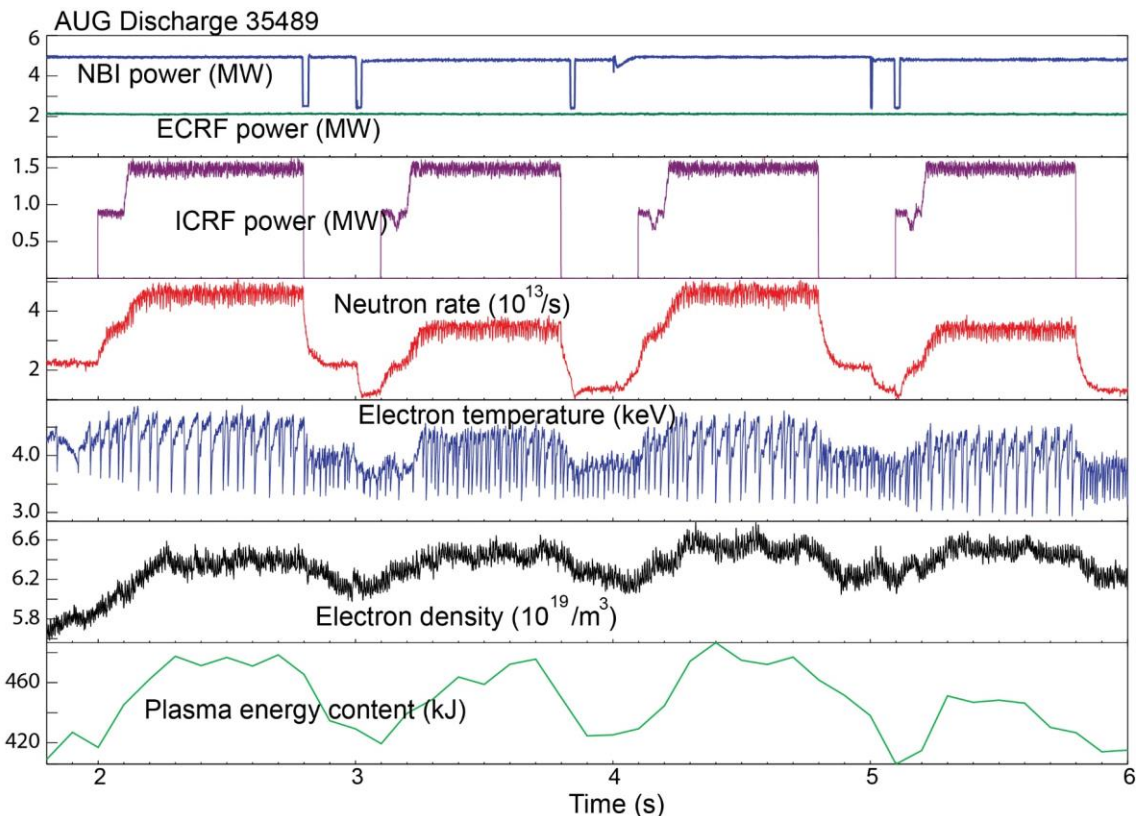


Fig. 9. Time evolution of NBI, ICRF and ECRF power, neutron rate, electron temperature, electron density and plasma energy content in AUG discharge 35489 with third harmonic ICRF heating of deuterium with synergy with D NBI. During the second and fourth ICRF phase, the energy of NBI injected deuterons was 60 keV while during the first and third ICRF phase, a combination of 60 and 93 keV deuterium beams was used.

## ACKNOWLEDGEMENTS

This work has been carried out within the framework of the EUROfusion Consortium and has received funding from the Euratom research and training programme 2014–2018 and 2019–2020 under grant agreement No 633053. The views and opinions expressed herein do not necessarily reflect those of the European Commission. O. Sauter was supported in part by the Swiss National Foundation.

## REFERENCES

- [1] CASSON F.J. et al. 2020 Nucl. Fusion 60, 066029.
- [2] MAILLOUX J. et al. to be published in Nuclear Fusion Special issue: Overview and Summary Papers from the 28<sup>th</sup> Fusion Energy Conference (Nice, France, 10-15 May 2021)
- [3] DUMONT R. et al. 2018 Nucl. Fusion 58, 082005
- [4] MANTSINEN M.J. et al. 2017 EPJ Web of Conferences 157, 03032.
- [5] BOBKOV V. et al. 2020 AIP Conference Proceedings 2254, 040005.
- [6] MANTSINEN M.J. et al. 2018 Europhysics Conference Abstracts, vol. 42A, P1.1072.
- [7] ERIKSSON, L.-G., HELLSTEN, T., WILLÉN, U., 1993 Nucl. Fusion 33, 1037.
- [8] BILATO R. et al. 2014, AIP Conference Proceedings 1580, 291.
- [9] MANTSINEN M.J. et al. 2015 AIP Conference Proceedings 1689, 030005.
- [10] DE OLIVEIRA N. et al. 2020, submitted to Nuclear Fusion.
- [11] DI SIENA A. et al 2019 Nucl. Fusion 59, 124001.
- [12] PÜTTERICH T. et al. 2018 27th IAEA Fusion Energy Conference (FEC2018), EX/P8-4
- [13] MANTSINEN M.J. et al., 2016 Europhysics Conference Abstracts, vol. 40A, P1.035.